

# Post exposure time dependence of deuterium retention in lithium and lithium compounds



Y. Yang<sup>a</sup>, L. Buzi<sup>a</sup>, A.O. Nelson<sup>b</sup>, R. Kaita<sup>c</sup>, B.E. Koel<sup>a,\*</sup>

<sup>a</sup> Department of Chemical and Biological Engineering, Princeton University, A311 EQuadrangle, Olden Street, Princeton, NJ 08544-5263, USA

<sup>b</sup> Department of Astrophysical Sciences, Princeton Program in Plasma Physics, Princeton University, Princeton, NJ 08544, USA

<sup>c</sup> Princeton Plasma Physics Laboratory, Princeton, NJ 08543-0451, USA

## ARTICLE INFO

### Keywords:

Deuterium retention  
Lithium  
Lithium compounds  
Time dependence

## ABSTRACT

Lithium (Li) coating of plasma-facing components (PFC) has led to improved plasma performance in fusion experiments due to the effectiveness of Li in retaining hydrogen (H) isotopes and thus reducing recycling. Since Li readily reacts with background gases present in fusion experiments, it is important to understand and parameterize the time dependence of deuterium (D) retention in Li and Li compounds for applications of Li under future long-pulse plasma conditions. D retention in pure Li and composite Li–O and Li–C–O films was studied as a function of time after these films were exposed to 450 eV  $D_2^+$  ion irradiation. The amount of deuterium retained in both Li and Li–O films at 300 K decreased at the same rate by 45% after 16 h. The amount of D retained in Li–C–O films was found to be independent of time up to 3 days. Increasing the temperature of a pure Li film to 420 K increased this rate of decrease by 50%, while increasing the thickness of the lithium film from 3 to 16 monolayers had no effect on the decrease rate.

## 1. Introduction

Lithium (Li) coating of plasma-facing components (PFCs) has led to improved plasma performance such as longer discharge time and higher current density in fusion experiments [1–6]. These effects have been attributed to the effectiveness of Li in reducing impurities in the plasma and retaining hydrogen (H) isotopes such as deuterium (D), thus reducing recycling [7–12]. Since Li readily reacts with background gases present in fusion devices, it is important to understand and parameterize D retention in both Li and Li compounds (Li–O and Li–C–O) for applications of Li under operating conditions. Furthermore, the evolution of D retention in the PFCs, i.e. the time dependent fuel retention property, is crucial under future long-pulse plasma conditions because of nuclear safety regulations related to tritium inventory in tokamaks [13, 14].

Several previous works have examined the effect of impurities on D retention in Li. Taylor et al. studied the effect of oxygen on D retention in lithiated graphite [15,16]. Capece et al. examined the effects of both temperature and contamination on D retention in ultrathin Li films on TZM [17]. Similarly, a few studies have addressed the time dependent fuel retention in PFCs. Bisson et al. [13] and Wierenga [18] have separately examined the retention of D in tungsten as a function of time. Ohno et al. have studied the time evolution of D in graphite [19]. Presently, no time dependent retention study on Li exists in the literature. This work extends

the existing literature on H retention by investigating D retention in Li and Li compounds (Li–O and Li–C–O) as a function of waiting time after exposure to 450 eV  $D_2^+$  ions. This is a critical step in addressing what happens to D trapped in Li PFCs between plasma shots, e.g., whether it diffuses out of the Li, stays trapped or forms other compounds.

## 2. Experimental methods

All experiments were performed in a three-level, stainless-steel UHV chamber ( $2 \times 10^{-10}$  Torr base pressure) equipped with Auger electron spectroscopy (AES) and temperature programmed desorption (TPD) capabilities, which enables the sample to be positioned for analysis by AES and TPD while fully remaining under UHV conditions. AES was performed with a PHI 15–255 G double-pass cylindrical mirror analyzer (CMA). TPD experiments were performed with the sample in line-of-sight of the ionizer of a shielded UTI 100C quadrupole mass spectrometer with the shield nozzle located 1 mm from the sample. The heating rate was 4 K/s. TPD was conducted monitoring these 12 masses: 2, 3, 4, 7, 9, 16, 18, 19, 20, 25, 28 and 32 amu. Surface coverages  $\theta$  are given in monolayers (ML), where 1 ML corresponds to the surface Ni atom density of Ni(110) ( $1.14 \times 10^{15}$  atoms/cm<sup>2</sup>).

A Ni(110) crystal (Princeton Scientific Corp, 8 mm square, 1 mm thick,  $\pm 0.5^\circ$  orientation) was used as the substrate for all experiments to

\* Corresponding author.

E-mail address: [bkoel@princeton.edu](mailto:bkoel@princeton.edu) (B.E. Koel).

<https://doi.org/10.1016/j.nme.2019.01.031>

Received 10 August 2018; Received in revised form 30 January 2019; Accepted 30 January 2019

Available online 01 March 2019

2352-1791/© 2019 Published by Elsevier Ltd. This is an open access article under the CC BY-NC-ND license

(<http://creativecommons.org/licenses/by-nc-nd/4.0/>).

avoid effects due to grain boundaries, intrinsic defects, and impurities diffusing to the surface [20]. The Ni(110) crystal was cleaned initially using 1.5 keV Ar<sup>+</sup> ion sputtering and annealing cycles at 1100 K. Additional oxygen treatments for several minutes at  $p(\text{O}_2) = 4 \times 10^{-8}$  Torr with the sample at 1000 K were used to eliminate residual carbon. Hydrogen treatments for several minutes at  $p(\text{H}_2) = 4 \times 10^{-8}$  Torr with the sample at 1000 K were used to eliminate residual oxygen. AES was used to establish that no additional cleaning was needed between experiments. Surface purity of the Ni(110) substrate prior to all experiments was determined with AES to ensure carbon and oxygen concentrations of less than 0.1%. A well-ordered surface was confirmed by low energy electron diffraction (LEED).

Li dosing was performed with a commercial Li metal dispenser (Li/NF/7.3/17/FT, SAES Group) by thermal evaporation onto the Ni substrate. The amount of Li dosed was calculated by integrating the total area under the subsequent Li TPD curve, corrected for the mass spectrometer sensitivity to the translational energy of the desorbed species [21]. The TPD area corresponding to  $\theta = 1$  ML has been defined previously [22]. As TPD is a destructive analysis technique, the Li film had to be redeposited for each retention time experiment, and this resulted in an experimental uncertainty of 8% (root mean square error) associated with the Li film thickness.

$\text{D}_2^+$  ions were produced in a PHI 04–303A differentially pumped ion gun with adjustable ion energy from 0–5 keV, and a liquid nitrogen trap was used in the  $\text{D}_2$  gas line to reduce  $\text{H}_2\text{O}$  contamination.  $\text{O}_2$  and CO (Praxair, 99.9%) was dosed through backfilling the chamber. Hydrogen impurities from background coadsorption in all deuterium experiments were less than 0.01 monolayers. All experiments were performed at 300 K unless otherwise noted.

Time-dependent D retention studies after Li dosing and  $\text{D}_2^+$  ion exposure, utilized different amounts of waiting time in the UHV environment prior to TPD and AES analysis. During the waiting time and sample movement for analysis, the sample was maintained at the UHV chamber base pressure of  $2 \times 10^{-10}$  Torr. Heating to 1350 K during TPD after  $\text{D}_2^+$  ion exposure restored the Ni substrate surface order and cleanliness, as confirmed by LEED and AES.

### 3. Results and discussion

#### 3.1. Time dependent D retention in Li

Three monolayers of Li were deposited onto the Ni substrate and subsequently irradiated with  $4 \times 10^{15} \text{ D}_2^+ \text{ cm}^{-2}$  at 450 eV. We

confirmed that the entire Li film was converted to LiD by the disappearance of a metallic multilayer Li peak in TPD (550–600 K) [22]. The LiD film was left undisturbed at 300 K for various amounts of time before being analyzed by AES and then by TPD.

$\text{D}_2$  TPD curves and AES spectra of the LiD film after different amounts of waiting time before analysis are shown in Fig. 1.  $\text{D}_2$  TPD curves show that  $\text{D}_2$  desorbed from a LiD decomposition-limited peak at 630 K [22]. With increasing amounts of waiting time, the 630 K peak decreased and a shoulder at 520 K grew. The 520 K shoulder occurred at a similar temperature to  $\text{D}_2$  desorption temperature from an oxidized Li film, discussed in Section 3.2, indicating that the LiD film could have been converted into Li oxide with increasing amounts of waiting time. The suggested conversion of Li to Li oxide was confirmed by the AES spectra, which showed a decrease in the metallic Li signal (51 eV) and an increase in the  $\text{Li}_2\text{O}$  signal (33 and 40 eV) and LiOD signal (45 eV) [23–26] over time.

The observed conversion of Li to Li oxide is a result of the Li film being oxidized by the residual water vapor ( $4 \times 10^{-11}$  Torr) in the UHV chamber during the long wait times for the experiments.

#### 3.2. Time dependent D retention in Li–O and Li–C–O

A Li oxide film was formed by first depositing three monolayers of Li onto the Ni substrate followed by backfilling the chamber with  $1 \times 10^{-7}$  torr of  $\text{O}_2$  for 5 min. Li oxide, which chemically could be  $\text{Li}_2\text{O}$  or  $\text{Li}_2\text{O}_2$ , shall be presented as Li–O in this work. We confirmed that the entire Li film was oxidized, converted to Li–O, by the disappearance of the metallic Li peak in AES (51 eV) and by the disappearance of a metallic multilayer Li peak in TPD (550–600 K) [22]. The Li–O film was subsequently irradiated with  $4 \times 10^{15} \text{ D}_2^+ \text{ cm}^{-2}$  at 450 eV. The  $\text{D}_2^+$  ion treated Li–O film was left undisturbed at 300 K for increasing amounts of waiting time before being analyzed by AES and then by TPD.

$\text{D}_2$  TPD curves and AES spectra of the  $\text{D}_2^+$  ion irradiated Li–O film after different amounts of waiting time before analysis are shown in Fig. 2.  $\text{D}_2$  TPD curves show that  $\text{D}_2$  desorbed from a single peak at 500 K. No LiD decomposition limited peak at 630 K was observed. With increasing waiting time, this 500 K peak decreased. No other TPD peaks were observed over time, indicating that the  $\text{D}_2^+$  ion treated Li–O film was chemically stable over time. This was confirmed by the AES spectra, which showed two peaks at 33 and 40 eV ( $\text{Li}_2\text{O}$  [24]) with no significant changes over time.

Twenty minutes of CO exposure at  $1 \times 10^{-7}$  Torr to a 3-layer Li film

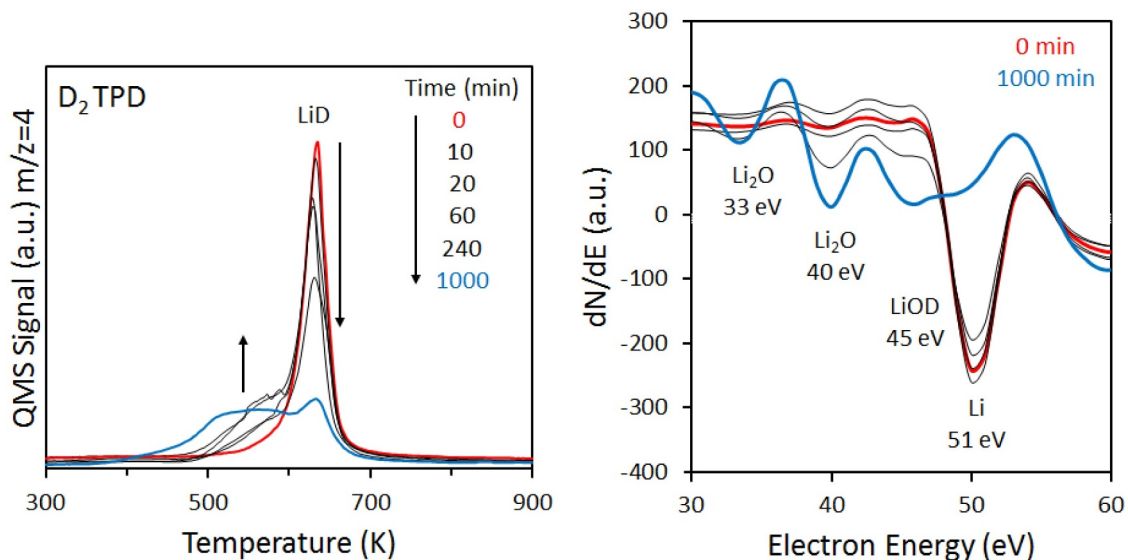


Fig. 1. TPD (left) and AES (right) of a 3-layer Li film irradiated with  $4 \times 10^{15} \text{ D}_2^+ \text{ cm}^{-2}$  at 450 eV for increasing amounts of waiting time at 300 K.

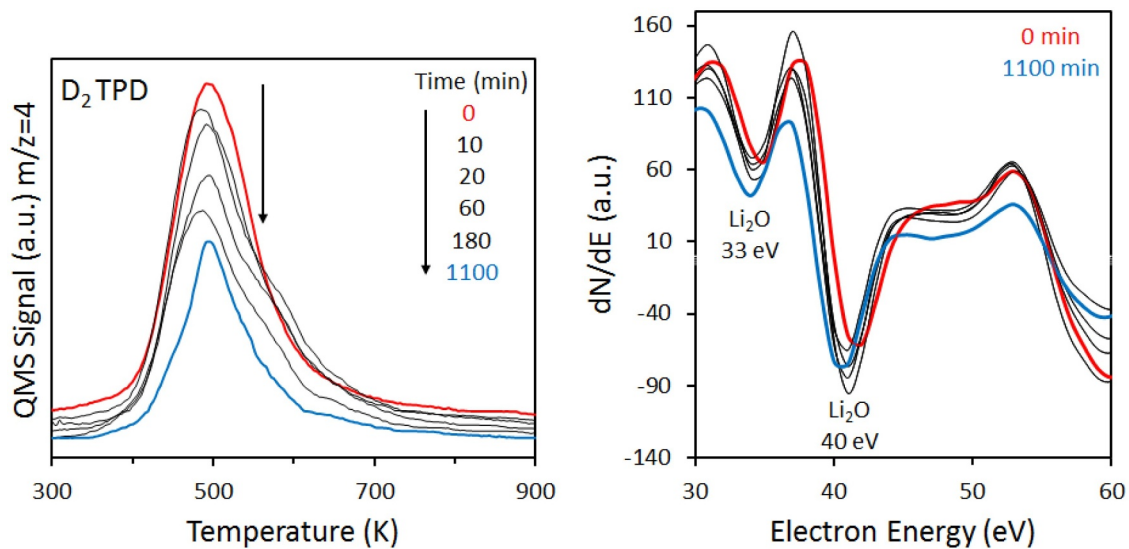


Fig. 2. TPD (left) and AES (right) of a 3-layer Li–O film irradiated with  $4 \times 10^{15} \text{ D}_2^+ \text{ cm}^{-2}$  at 450 eV for increasing amounts of waiting time at 300 K.

led to the formation of a mixed Li–C–O composite surface. We confirmed that the entire Li film was converted to Li–C–O by the disappearance of the metallic Li peak in AES (51 eV). The Li–C–O composite film was subsequently irradiated with  $4 \times 10^{15} \text{ D}_2^+ \text{ cm}^{-2}$  at 450 eV. The  $\text{D}_2^+$  ion treated Li–C–O film was left undisturbed at 300 K for increasing amounts of time before being analyzed by AES and then by TPD.

$\text{D}_2$  TPD curves and AES spectra of the  $\text{D}_2^+$  irradiated Li–C–O film after different amounts of waiting time before analysis are shown in Fig. 3.  $\text{D}_2$  TPD curves show that  $\text{D}_2$  initially desorbed from two peaks at 500 and 550 K. No LiD decomposition limited peak at 630 K was observed. With increasing waiting time, the 550 K peak decreased and diminished while the 500 K peak grew. No other TPD peaks were observed. The AES spectra showed a small decrease in the LiOD signal (45 eV), but showed no significant changes in  $\text{Li}_2\text{O}$  signals (33 and 40 eV) over time.

### 3.3. Summary and comparison to literature

The  $\text{D}_2$  retention fraction as a function of time is plotted in Fig. 4. The retention fraction of  $\text{D}_2$  is defined here as the integrated  $\text{D}_2$  TPD

area at various waiting times divided by the integrated  $\text{D}_2$  TPD area at 1 min waiting time.

In addition to the results of the three experiments discussed in Section 3.1 and 3.2, the results of two more experiments are included in Fig. 4. First, labeled as Li (16 ML, 300 K), 16 layers of Li were deposited onto the Ni substrate and subsequently irradiated with  $8 \times 10^{15} \text{ D}_2^+ \text{ cm}^{-2}$  at 450 eV. This thicker Li film was left undisturbed at 300 K for increasing amounts of time before being analyzed by AES and then by TPD. Second, labeled as Li (3 ML, 420 K), 3 layers of Li were deposited onto the Ni substrate and subsequently irradiated with  $4 \times 10^{15} \text{ D}_2^+ \text{ cm}^{-2}$  at 450 eV. This Li film was left undisturbed at 420 K for increasing amounts of time before being analyzed by AES and then by TPD.

Furthermore, the time dependent  $\text{D}_2$  retention results at room temperature on tungsten by Bisson et al. [13] and Wierenga [18] and on graphite by Ohno et al. [19] are included for comparison.

The  $\text{D}_2$  retention fraction in the 3-layer Li film (black circle), 16-layer Li film (square) and 3-layer Li–O film (triangle) at 300 K decreased at similar rates to a final value of 0.5–0.6 after 1000 min. Li and Li–O films exhibit similar  $\text{D}_2$  retention as a function of time, likely due to the fact that Li was converted to Li oxide during the waiting time, as

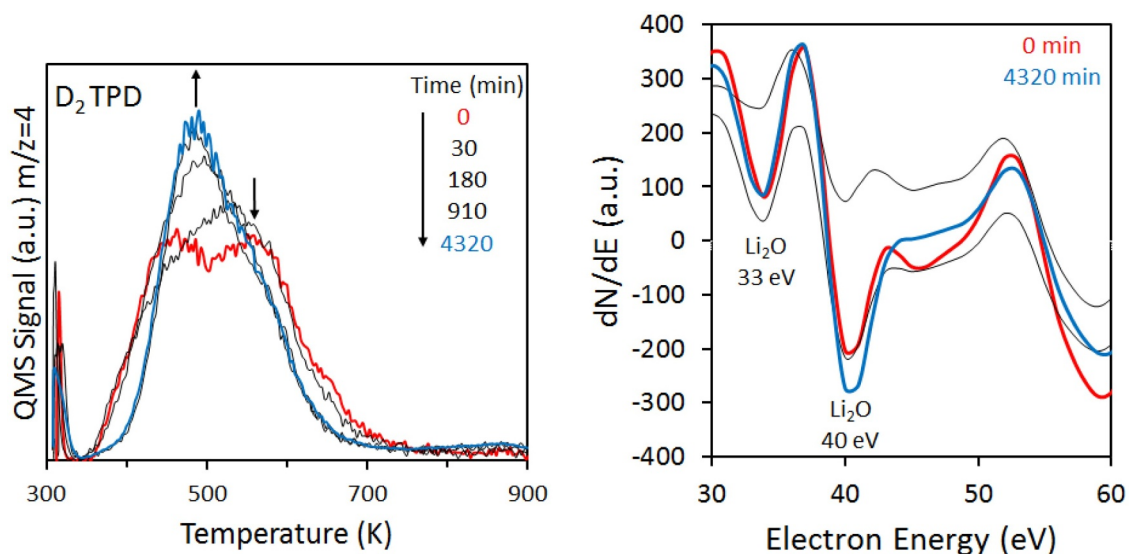


Fig. 3. TPD (left) and AES (right) of a 3-layer Li–C–O film irradiated with  $4 \times 10^{15} \text{ D}_2^+ \text{ cm}^{-2}$  at 450 eV for increasing amounts of waiting time at 300 K.

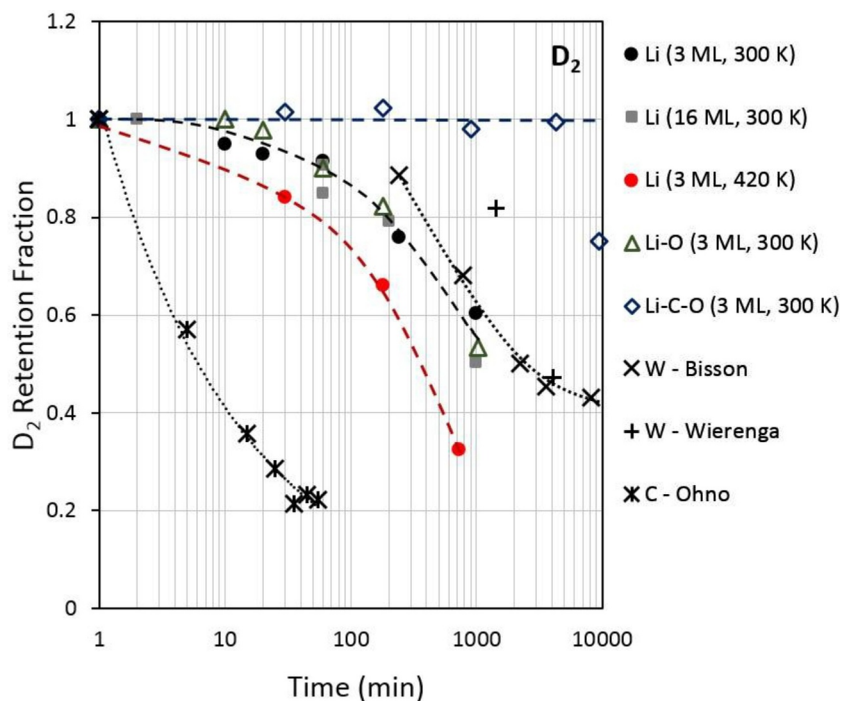


Fig. 4.  $D_2$  retention fraction of as a function of time after exposure of  $D_2^+$  on Li, Li–O and Li–C–O films. Literature results of  $D_2$  retention fraction on tungsten [13,18] and graphite [19] over time are also included for comparison. Lines are drawn to guide the eye.

discussed in Section 3.1. The  $D_2$  retention fraction in the 3-layer Li film at 420 K (red circle) decreased at a faster rate to a final value of 0.32 after 730 min. This faster rate of decrease at higher temperature can be explained if the loss mechanism of  $D_2$  from Li and Li–O films is physical diffusion.

$D_2$  retention in the 3-layer Li–C–O film was found to be independent of time up to 4320 min (3 days). The  $D_2$  retention fraction in the 3-layer Li–C–O film eventually decreased to 0.75 after 9360 min (6.5 days). Clearly, the Li–C–O has an altered the loss mechanism for  $D_2$  retained in these Li compounds.

Comparing these results to  $D_2$  retention in tungsten and graphite, it can be seen that at 300 K, the  $D_2$  retention fraction decreased fastest in graphite over time, followed by Li and Li–O, and then tungsten. The  $D_2$  retention fraction decreased slowest in Li–C–O.

The amount of Li was observed to be independent of the time after exposure of  $D_2^+$ , as determined by Li TPD (not shown here). This is expected since Li does not evaporate significantly below 420 K on the timescale of these experiments and Li is reversibly adsorbed and thus fully desorbs without loss of Li into the Ni substrate [20].

#### 4. Conclusions

$D_2$  retention in pure Li and Li compound (Li–O and Li–C–O) films has been studied as a function of time after these films were exposed to 450 eV  $D_2^+$  ion irradiation. The amount of  $D_2$  retained in both Li and Li–O films at 300 K decreased at similar rates by 45% after 16 h, likely due to Li being oxidized to Li oxide during the waiting time. The retention in Li–C–O films was found to be independent of time up to three days. Increasing the temperature of the Li film to 420 K increased this rate of decrease, which can be explained if the  $D_2$  loss mechanism from Li film is physical diffusion. Comparing to literature results of  $D_2$  retention in other materials at 300 K, the  $D_2$  retention capability of Li and Li–O over time falls between graphite (which loses  $D_2$  faster) and tungsten (which loses  $D_2$  slower).

#### Declaration of interest

None.

#### Acknowledgments

This material is based upon work supported by the U.S. Department of Energy, Office of Science/Fusion Energy Sciences under Award DESC0012890 and by the Program in Plasma Science and Technology (PPST) at Princeton University. YY acknowledges support by the Program in Plasma Science and Technology (PPST) at Princeton University.

#### Supplementary materials

Supplementary material associated with this article can be found, in the online version, at [doi:10.1016/j.nme.2019.01.031](https://doi.org/10.1016/j.nme.2019.01.031).

#### References

- [1] M.G. Bell, H.W. Kugel, R. Kaita, L.E. Zakharov, H. Schneider, B.P. LeBlanc, D. Mansfield, R.E. Bell, R. Maingi, S. Ding, S.M. Kaye, S.F. Paul, S.P. Gerhardt, J.M. Canik, J.C. Hosea, G. Taylor, The NSTX Research Team, Plasma response to lithium-coated plasma-facing components in the National Spherical Torus Experiment, *Plasma Phys. Control. Fusion* 51 (2009) 124054.
- [2] S. Mirnov, V. Lazarev, S. Sotnikov, Li-CPS limiter in tokamak T-11M, *Fusion Eng. Des.* 65 (2003) 455–465.
- [3] J. Sanchez, F.L. Tabare's, D. Tafalla, J.A. Ferreira, I. Garcia-Cortes, C. Hidalgo, F. Medina, M.A. Ochando, M.A. Pedrosa, TJ-II Team, Impact of lithium-coated walls on plasma performance in the TJ-II stellarator, *J. Nucl. Mater.* 390–391 (2009) 852–857.
- [4] A. Tuccillo, A. Alekseyev, B. Angelini, S.V. Annibaldi, M. Apicella, G. Apruzzese, J. Berrino, E. Barbato, A. Bertocchi, A. Biancalani, Overview of the FTU results, *Nucl. Fusion* 49 (2009) 104013.
- [5] G. Xu, B. Wan, J. Li, X. Gong, J. Hu, J. Shan, H. Li, D. Mansfield, D. Humphreys, V. Naulin, Study on H-mode access at low density with lower hybrid current drive and lithium-wall coatings on the EAST superconducting tokamak, *Nucl. Fusion* 51 (2011) 072001.
- [6] S. Munaretto, S. Dal Bello, P. Innocente, M. Agostini, F. Auriemma, S. Barison, A. Canton, L. Carraro, G. De Masi, S. Fiameni, P. Scarin, D. Terranova, RFX-mod wall conditioning by lithium pellet injection, *Nucl. Fusion* 52 (2012) 023012.
- [7] C.H. Skinner, J.P. Allain, W. Blanchard, H.W. Kugel, R. Maingi, L. Roquemore, V. Soukhanovskii, C.N. Taylor, Deuterium retention in NSTX with lithium conditioning, *J. Nucl. Mater.* 415 (2011) S773–S776.
- [8] J.P. Allain, C.N. Taylor, Lithium-based surfaces controlling fusion plasma behavior at the plasma-material interface, *Phys. Plasmas* 19 (2012) 056126.
- [9] R. Kaita, M. Lucia, J.P. Allain, F. Bedoya, R. Bell, D. Boyle, A. Capece, M. Jaworski, B.E. Koel, R. Majeski, J. Roszell, J. Schmitt, F. Scotti, C.H. Skinner, V. Soukhanovskii, Hydrogen retention in lithium on metallic walls from “in vacuo” analysis in LTX and implications for high-Z plasma-facing components in NSTX-U,

- Fusion Eng. Des. 117 (2017) 135–139.
- [10] C.N. Taylor, K.E. Luitjohan, B. Heim, L. Kollar, J.P. Allain, C.H. Skinner, H.W. Kugel, R. Kaita, A.L. Roquemore, R. Maingi, Surface chemistry analysis of lithium conditioned NSTX graphite tiles correlated to plasma performance, *Fusion Eng. Des.* 88 (2013) 3157–3164.
- [11] P.S. Krstic, J.P. Allain, C.N. Taylor, J. Dadras, S. Maeda, K. Morokuma, J. Jakowski, A. Allouche, C.H. Skinner, Deuterium uptake in magnetic-fusion devices with lithium-conditioned carbon walls, *Phys. Rev. Lett.* 110 (2013) 105001.
- [12] M.J. Baldwin, R.P. Doerner, S.C. Luckhardt, R.W. Conn, Deuterium retention in liquid lithium, *Nucl. Fusion* 42 (2002) 1318–1323.
- [13] R. Bisson, S. Markelj, O. Mourey, F. Ghiorghiu, K. Achkasov, J.-M. Layet, P. Roubin, G. Cartry, C. Grisolia, T. Angot, Dynamic fuel retention in tokamak wall materials: an in situ laboratory study of deuterium release from polycrystalline tungsten at room temperature, *J. Nucl. Mater.* 467 (2015) 432–438.
- [14] S. Brezinsek, T. Loarer, V. Philipps, H.G. Esser, S. Grünhagen, R. Smith, R. Felton, J. Banks, P. Belo, A. Boboc, J. Bucalossi, M. Clever, J.W. Coenen, I. Coffey, S. Devaux, D. Douai, M. Freisinger, D. Frigione, M. Groth, A. Huber, J. Hobirk, S. Jachmich, S. Knipe, K. Krieger, U. Kruezi, S. Marsen, G.F. Matthews, A.G. Meigs, F. Nave, I. Nunes, R. Neu, J. Roth, M.F. Stamp, S. Vartanian, U. Samm, J.E. Contributors, Fuel retention studies with the ITER-Like Wall in JET, *Nucl. Fusion* 53 (2013) 083023.
- [15] C.N. Taylor, J. Dadras, K.E. Luitjohan, J.P. Allain, P.S. Krstic, C.H. Skinner, The role of oxygen in the uptake of deuterium in lithiated graphite, *J. Appl. Phys.* 114 (2013) 223301.
- [16] C.N. Taylor, J.P. Allain, K.E. Luitjohan, P.S. Krstic, J. Dadras, C.H. Skinner, Differentiating the role of lithium and oxygen in retaining deuterium on lithiated graphite plasma-facing components, *Phys. Plasmas* 21 (2014) 057101.
- [17] A.M. Capece, J.P. Roszell, C.H. Skinner, B.E. Koel, Effects of temperature and surface contamination on D retention in ultrathin Li films on TZM, *J. Nucl. Mater.* 463 (2015) 1177–1180.
- [18] H. Wierenga, Modelling Diffusion Processes of Deuterium in Tungsten, Faculty of Science Theses, Utrecht University, 2013.
- [19] N. Ohno, Y. Nakamura, M. Yamagiwa, T. Kaneko, N. Matsunami, S. Kajita, M. Takagi, In situ measurement of deuterium retention in graphite under successive exposure to deuterium and hydrogen plasmas, *Phys. Scr.* T159 (2014) 014053.
- [20] V. Saltas, C.A. Papageorgopoulos, Adsorption of Li on Ni(110) surfaces at low and room temperature, *Surf. Sci.* 461 (2000) 219–230.
- [21] Y. Tsai, C. Xu, B.E. Koel, Chemisorption of ethylene, propylene and isobutylene on ordered Sn/Pt(111) surface alloys, *Surf. Sci.* 385 (1997) 37–59.
- [22] L. Buzi, Y. Yang, F.J. Domínguez-Gutiérrez, A.O. Nelson, M. Hofman, P.S. Krstić, R. Kaita, B.E. Koel, Hydrogen retention in lithium and lithium oxide films, *J. Nucl. Mater.* 502 (2019) 161–168.
- [23] J. Engbæk, G. Nielsen, J. H. Nielsen, I. Chorkendorff, Growth and decomposition of lithium and lithium hydride on nickel, *Surf. Sci.* 600 (2006) 1468–1474.
- [24] J.P. Tonks, M.O. King, E.C. Galloway, J.F. Watts, Corrosion studies of LiH thin films, *J. Nucl. Mater.* 484 (2017) 228–235.
- [25] R.E. Clausing, D.S. Easton, G.L. Powell, Auger spectra of lithium metal and lithium oxide, *Surf. Sci.* 36 (1973) 377–379.
- [26] C.F. Mallinson, J.E. Castle, J.F. Watts, Analysis of the Li KLL auger transition on freshly exposed lithium and lithium surface oxide by AES, *Surf. Sci. Spec.* 20 (2013) 113–127.